

1 SIO 217A: ROAST Project 2014
2 Radiative Cloud Study
3
4

5 **Mid-Latitude Cirrus Thinning and Thickening:**
6 **A Radiative Sensitivity Study**
7

8 ¹**Dillon Amaya**, ¹**Reuben Demirdjian**, and ¹**Alan Seltzer**

9 ¹Scripps Institution of Oceanography, 8622 Kennel Way, La Jolla, CA 92037
10
11
12
13
14
15
16
17
18
19
20
21
22
23
24
25
26
27
28
29
30
31
32
33
34
35
36
37
38

39 1. INTRODUCTION

40
41 Global average surface air temperature (SAT) has been significantly increasing since the
42 industrial revolution [Trenberth *et al.*, 2007]. This has led the scientific community to focus their
43 efforts on understanding how and why climate will be impacted by such a change. Additionally,
44 considerable resources have been dedicated to geoengineering the large-scale climate to reduce
45 global warming. Solar radiation management is widely considered by the Intergovernmental
46 Panel on Climate Change as a viable option.

47 Solar radiation management attempts to manipulate the amount of solar radiation incident on
48 the Earth's surface to manage global average SAT. Large amounts of absorption at the surface of
49 shortwave radiation will increase SATs. In turn this will increase outgoing longwave radiation
50 emitted by the Earth, which will cause higher absorption of greenhouse gases. These gases will
51 re-emit in all directions thereby further increasing the amount of longwave radiation absorbed at
52 the surface. Proposed efforts to manage the amount of incoming solar radiation range from
53 increasing cloud albedos [Latham, 2002] to obstructing solar radiation with space-based mirrors
54 [Bewick *et al.*, 2012]. In the context of manipulating cloud albedo, special consideration has been
55 given to cirrus clouds.

56 Cirrus clouds are mainly composed of ice crystals and have temperatures ranging from
57 ~185K-210K. Such clouds tend to be found between 8-20km with an average cloud depth of
58 4.5km [Orikasa *et al.*, 2013]. Due to the large concentration of ice crystals found in cirrus
59 clouds, the optical and radiative properties are non-trivial as they depend on the size, shape, and
60 orientation of ice crystals. In general, cirrus clouds have high albedo and are effective at
61 reflecting shortwave radiation, which acts as cooling effect on climate. Ice-crystals can also be
62 strong absorbers of longwave radiation and therefore act as a warming effect on climate. Thus,
63 geoengineering research has been aimed at maximizing the albedo of cirrus clouds while
64 reducing the relative amount of longwave radiation absorbed. In this project, we use observed
65 ice-crystal particle size distributions in a mid-latitude cirrus cloud in an attempt to find this
66 "goldilocks zone" and improve our understanding of the relative role cirrus clouds play in the
67 climate system.

68

69 2. METHODS: MODEL, OBSERVATIONAL DATA, & ASSUMPTIONS

70
71 The number concentrations of the ice crystals reported by [Orikasa *et al.*, 2013] come from a
72 series of 37 mid-latitude cirrus ballooning experiments from the periods of 1994 to 2007. The ice
73 crystal imaging system on board the balloons payload is the hydrometeor videosonde or HYVIS.
74 The HYVIS instrument is capable of measuring ice crystals with radii of 10 μm to 200 μm with
75 uncertainties of a factor of 3 from 10-30 μm and of a factor of 2 above 30 μm .

76 The data of the HYVIS instrument is given on a scatter plot of the number concentration, in
77 units of $\text{m}^{-3}\mu\text{m}^{-1}$, versus the maximum dimension, in units of μm . Since the number
78 concentration is normalized by the bin size of the ice crystal sizes, it is required to multiply the
79 concentration by the bin size to get the true concentrations [e.g., Seinfeld and Pandis, 2006]. The
80 maximum dimension quantity is used in place of radius because ice crystals are non-spherical.

81 However, due to the enormous level of added complexity in determining the radiative properties
 82 of the actual shape of ice crystals, for the purpose of this study we are assuming ice crystals to
 83 completely spherical and the maximum dimension to be the radius.

84 Given the particle size distribution the ice water path and effective radius can be determined
 85 by a series of intermediate steps. From here, the optical depth can be calculated. For brevity we
 86 do not show the equations describing ice water path, effective radius, or optical depth. The full
 87 derivations can be found in *Thermodynamics of Atmospheres and Oceans*, [1999]. Upon
 88 calculating the optical depth of the cirrus cloud, the shortwave absorptivity can be calculated
 89 using the methods presented by [Ramswamy *et al.*, 1989]. It is important to constrain shortwave
 90 absorptivity because it can be used as an intermediate step to calculated reflectivity. If
 91 absorptivity (A) and transmissivity (T) are known then reflectivity (R) is:

$$92 \quad \quad \quad R = 1 - A - T \quad (1)$$

93 where,

$$94 \quad \quad \quad T = e^{-\tau \cdot \sec Z} \quad (2)$$

95 and

$$96 \quad \quad \quad A(\mu, \tau) = 0.5(0.346 + 0.234F_1 - 0.076F_2 + 0.014F_3) \\ 97 \quad \quad \quad + K_2(0.267 + 0.048F_1 - 0.012F_2 - 0.006F_3) + K_3(-0.006 - 0.005F_1 + 0.005F_2 - 0.005F_3) \quad (3)$$

98 where,

$$99 \quad \quad \quad \mu = \cos(z), \quad z = \text{zenith angle}; \quad \quad \quad F_1 = 0.1\tau - 1; \\ 100 \quad \quad \quad \tau = \text{optical depth}; \quad \quad \quad F_2 = 2F_1^2 - 1; \\ 101 \quad \quad \quad K_2 = (2\mu - 1.01)/0.99; \quad \quad \quad F_3 = 4F_1^3 - 3F_1; \\ 102 \quad \quad \quad K_3 = (2K_2^2 - 1);$$

103 It is important to note that this absorptivity is defined for a specific optical depth range of $0.5 < \tau$
 104 < 20 . The values for the incoming shortwave radiation and the outgoing longwave radiation were
 105 derived for a latitude of 45° . The shortwave mid-latitude solar radiance is given approximately
 106 by,

$$107 \quad \quad \quad F_{\text{short}} \approx 0.42 \cdot S_0 \cdot \sin(45^\circ) \approx 400 \text{ W/m}^2 \quad (4)$$

108 where,

$$109 \quad \quad \quad S_0 = 1360 \text{ W/m}^2 \text{ (Solar constant)} \quad (5)$$

110 Equation 4 is evident as about 42% of incoming solar spectrum is in the shortwave.
 111 Therefore, we only take into account 42% of the total incident solar radiation at 45° latitude. The
 112 longwave radiance value used is 230 W/m^2 , which comes from the NOAA climatological table
 113 of outgoing longwave radiation (OLR). The troposphere contains nearly 100% of the water vapor
 114 found in the atmosphere. Further, water vapor has been shown to be the primary absorber of
 115 OLR (REFERENCE). Therefore, full atmosphere OLR can be estimated by measuring OLR out
 116 of the top of the troposphere. Cirrus clouds are predominantly found near or above the

121 tropopause. As a result, the incoming longwave radiation measured at the bottom of a cirrus
 122 cloud can be used as an approximation for full atmosphere OLR.

123 We then were able to scale the relative particle size concentration and begin our sensitivity
 124 tests. Each scaling of particle size concentration had unique values for shortwave and longwave
 125 reflectivity and absorptivity. Total reflected upward shortwave fluxes and total emitted
 126 downward longwave fluxes were calculated for each iteration (each scaling). A change in total
 127 upward shortwave flux and a change total downward longwave flux, relative to the value for the
 128 original particle size distribution, was calculated for each iteration. Then, the difference between
 129 these changes at each iteration was taken as a net warming or net cooling and plotted in the
 130 figures below (Figures 2, 5, and 6). For example, if there was a larger increase in total shortwave
 131 reflectance than increase in total longwave absorption, there was a net cooling.

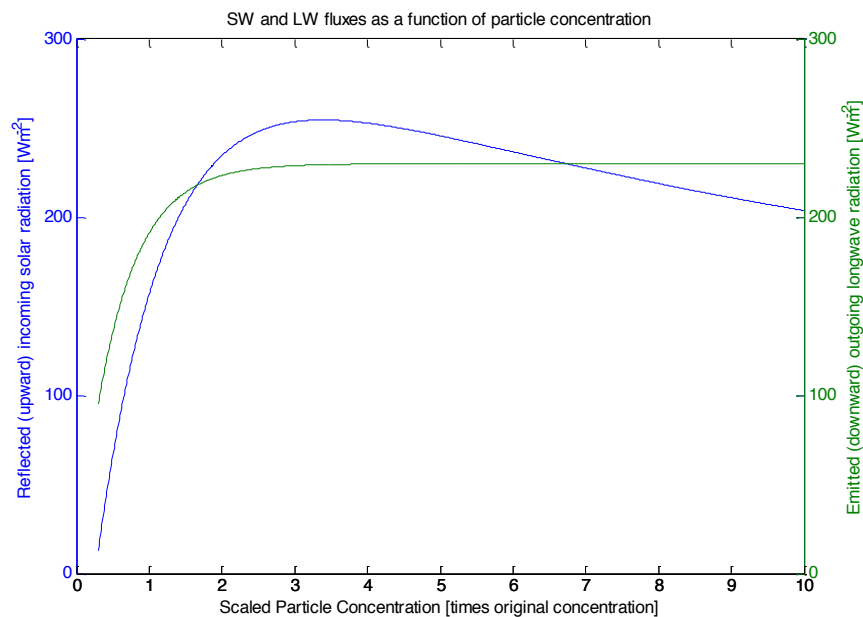
132

133 3. RESULTS

134

135 We present results for our initial sensitivity study, run with the following model conditions:
 136 assumed average cirrus cloud thickness of 4000m, zenith angle of 0° , and OLR and F_{short} as
 137 approximated for 45° N or S latitude as in Section 2. Figure 1 shows upward reflected SW
 138 radiation and downward absorbed (and emitted) LW radiation as a function of cloud thinning or
 139 seeding (i.e. scaled particle concentration). Reflectivity in the SW spectrum increases with cloud
 140 particle density up to a threshold, but then decreases. LW absorptivity under these conditions
 141 reaches 100% at around three times the measured cloud density used in our sensitivity study.

142

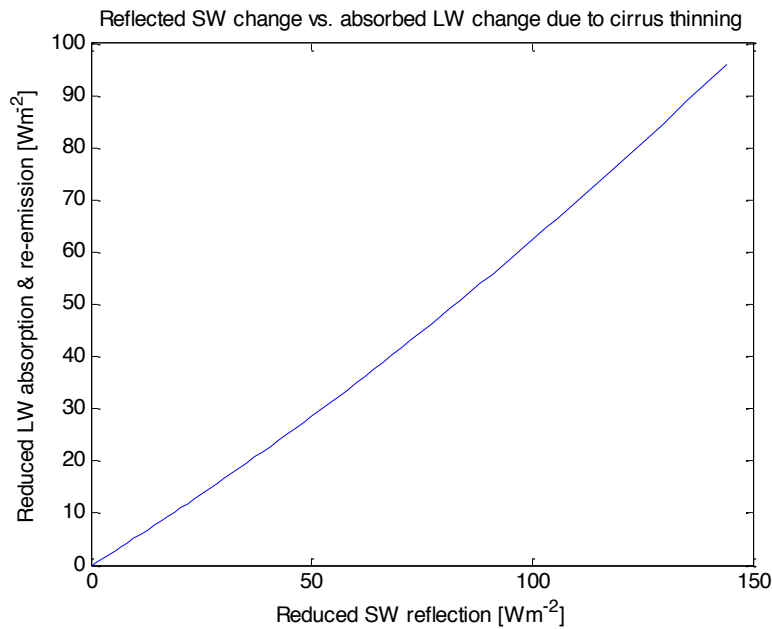


143

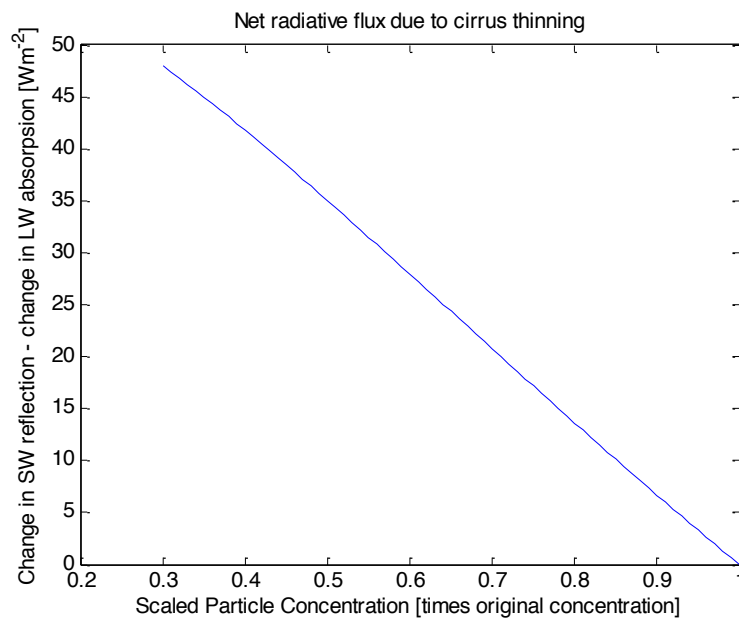
144 **Figure 1:** SW reflected and LW emitted fluxes for degrees of thinning/thickening

145

146 To determine the ideal degree (scaling) of thickening or thinning the cloud via addition or
 147 removal of particles, we performed two separate analyses: one for thinning and one for
 148 thickening. When we considered only the thinning, we found that for these assumed conditions
 149 (zenith angle of 0° and cloud thickness of 4000m) no amount of thinning would lead to a net
 150 cooling effect. That is, there is no scalar below one that, when multiplied by the initial particle
 151 distribution, would lead to a larger decrease in LW absorption than SW reflection. Figures 2 and
 152 3 show the radiative effects of thinning.

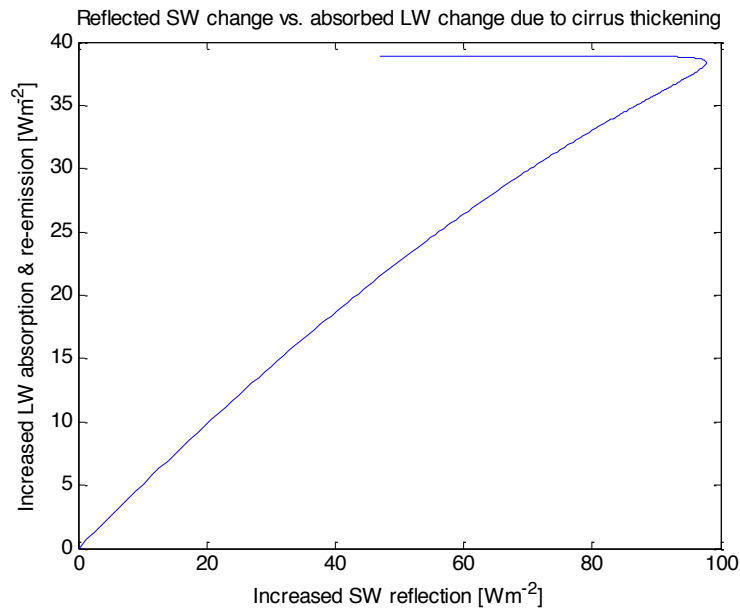


153 **Figure 2:** Reduction in SW reflection associated with reduction in LW absorption for thinning
 154
 155

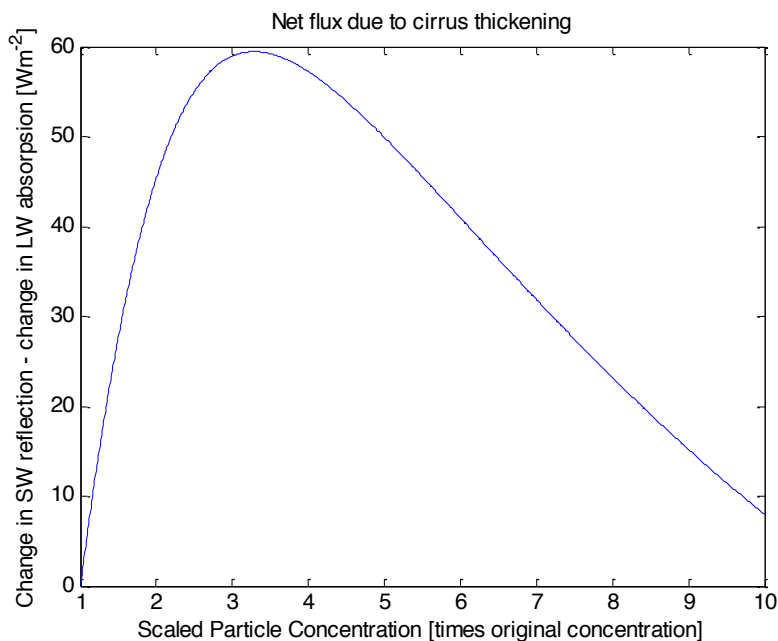


156 **Figure 3:** Net radiative flux for cirrus thinning. All values are positive and indicate net warming.
 157
 158

159 For the second analysis, we considered only cirrus thickening. By increasing the number of
 160 particles in the cloud, the net change in total reflected incoming SW exceeded the net change in
 161 total emitted LW. That is, for all thicker clouds (1-10 times the original size concentration), there
 162 was a net cooling effect. Figures 4 and 5 illustrate this finding. However, by extending the range
 163 of maximum particle density scaling, there appears to be a threshold at which increased LW
 164 emission is larger than increased SW reflection before reflection dominates once again, as shown
 165 in Figure 6.



166
 167 **Figure 4:** Relationship between increased SW reflection and LW emission for thickening.
 168



169
 170 **Figure 5:** Net radiative flux for cirrus thickening. All values are positive and indicate net
 171 warming. Maximum cooling is achieved at 3.29 times the original particle density.

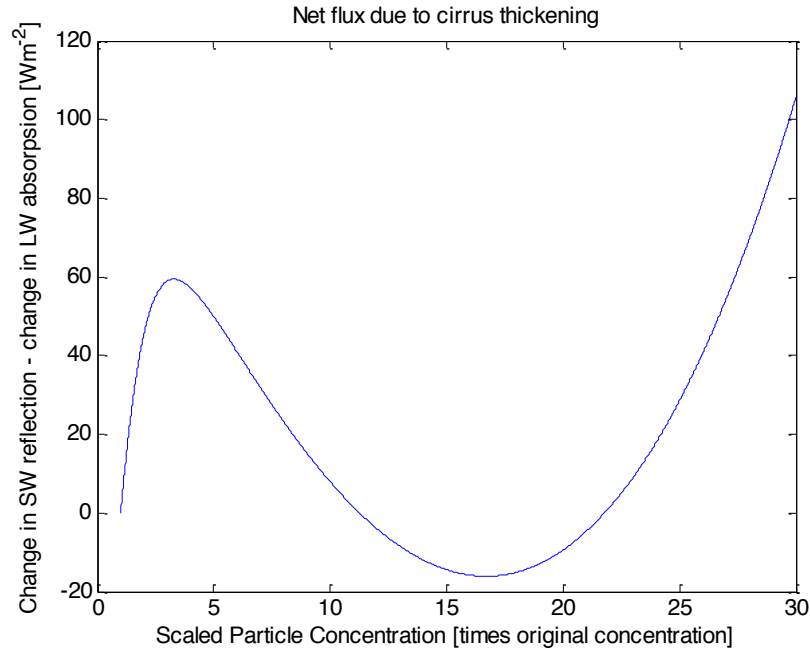


Figure 6: Net radiative flux for cirrus thickening after extending the particle density scaling range. Emission changes dominate reflection changes (net warming) from scalars of ~ 10 to 23.

4. CONCLUSIONS

In this study, we separately consider thinning and thickening of the cirrus cloud described by [Orikasa *et al.*, 2013] by decreasing the particle density to 0.3 times the original value to increasing the number of particle density tenfold. We considered net changes in total upward incoming SW reflection and downward outgoing LW absorption and emission. We consider a tenfold increase in the cloud particle density to be an upper bound on geoengineering possibilities, thus making a 30-fold increase as in Figure 6 unlikely.

Under our initial assumptions about the zenith angle and average cloud thickness, we found that a 3.29 times increase in the particle density of this particular cirrus cloud would maximize cooling. However, the zenith angle and cloud thickness play important roles in the radiative properties of clouds. Modifying them in this sensitivity study showed substantial changes in our maximal cooling outcomes.

Further analysis might include sensitivity of net radiative fluxes to altering the cloud depth, zenith angle, and assumed SW and LW fluxes coming into the cloud.

5. REFERENCES

1. Ebert, E.E. and J.A. Curry, 1992: A parameterization of cirrus cloud optical properties for climate models. *J. Geophys. Res.*, **97**, 3831-3836.
2. Orikasa, N., M. Murakami, and A.J. Heymsfield, 2013: Ice crystal concentration in midlatitude cirrus clouds: In situ measurements with the balloonborne hydrometeor videosonde (HYVIS). *J. of the Meteor. Soc. of Japan*, **91**, 143-161, doi: 10.2151/jmsj.2013-204.
3. Ramaswamy, V. and V. Ramanathan, 1989: Solar absorption by cirrus clouds and the maintenance of the tropical upper troposphere thermal structure. *J. of the Atmo. Sci.* 46:2293-2310.
4. Curry, J. A., and P. J. Webster, 1999: Thermodynamics of the Atmospheres and Oceans. Academic Press. Chapter 8.
5. Bewick, R., J. P. Sanchez, and C. R. McInnes, 2012: Gravitationally bound geoengineering dust shade at the inner Lagrange point. *Adv. in Space Res.* **50** (10): 1405. doi:10.1016/j.asr.2012.07.008
6. Latham, J., 2002: Amelioration of global warming by controlled enhancement of the albedo and longevity of low-level maritime clouds. *Atmo. Sci. Lett.* **3** (2–4): 52. doi:10.1006/asle.2002.0048
7. Seinfeld, John H., and Spyros N. Pandis. Atmospheric Chemistry and Physics from Air Pollution to Climate Change. 2nd ed. New York: Wiley, 2006.
8. Cess, R. D., 1974: Radiative Transfer Due to Atmospheric Water Vapor: Global Considerations of the Earth's Energy Balance. *J. Q.S.R.T.*, **14.9**, 861-71.